Civil Engineering and Applied Solutions

Research Article

journal homepage: ceas.journals.umz.ac.ir

CEAS Civil Engineering and Applied Solutions

Damage Identification in Truss Structures Using a Hybrid PSO-HHO Algorithm with Selective Natural Frequencies and Mode Shape

Sayyed Hadi Alavi [a], Amirhossein Pilehvaran [a], Mohammadreza Mashayekhi [a*]

[a] *Civil Engineering Department, K.N. Toosi University of Technology, Tehran, Iran*

ARTICLE INFO

Keywords:
Structural damage detection
Modal parameters
Hybrid PSO-HHO algorithm
Inverse problem

Article history:
Received 25 May 2025
Accepted 13 June 2025
Available online 1 July 2025

ABSTRACT

Structural damage can be detected non-destructively by comparing the dynamic characteristics of a structure before and after a major event. Optimization techniques are effective tools for damage identification using structural dynamic properties, as the problem is formulated and solved inversely. To achieve this, the damage levels in each element are treated as decision variables. The objective is to fine-tune these variables so that the model's response closely aligns with the experimentally observed dynamic characteristics of the damaged structure. This study proposes a hybrid Particle Swarm optimization- Harris Hawks optimization algorithm for damage detection in truss structures based on dynamic structural responses. To evaluate the effectiveness of the proposed method, two case study of planar truss is considered as a numerical examples. The results highlight the importance of incorporating modal parameters to accurately identify the damage scenario. The results demonstrate that the hybrid algorithm significantly outperforms the individual algorithms in accurately detecting structural damage.

1. Introduction

Structures may sustain damage during their service life due to various factors, including corrosion, deterioration, excessive loading, and construction errors [1]. Damages may obvious as changes in the structural stiffness or effective mass, potentially leading to disruptions in the structural performance. Proper inspection, monitoring, and maintenance of structures are essential to ensure economic efficiency and promote sustainability in engineering [2,3]. Damage detection is considered the initial stage of a broader process known as damage identification [4]. Non-destructive damage detection methods identify structural damage without causing damage to the structure, utilizing its dynamic characteristics. Compared to destructive techniques, these methods are safer, more cost-effective, and better suited for continuous structural monitoring [5]. Non-destructive methods are primarily implemented through analytical approaches. For years, researchers have been investigating non-destructive techniques for damage identification. In general, when a structural member is damaged, the resulting changes directly influence the stiffness matrix of the structure, leading to alterations in its vibrational behavior [6]. For this reason, one of the effective approaches in non-destructive structural damage identification is to examine changes in the dynamic properties of the structure by utilizing natural frequencies and mode shapes [7,8]. On the other hand, various structural responses can be used as damage indicators, but modal parameters have the advantage of being independent of external excitation [9].

The first studies on damage identification based on monitoring changes in natural frequencies are conducted by Adams et al. [10,11]. They found that natural frequencies are highly dependent on the overall stiffness and mass distribution of the structure; therefore, even minor damages can cause measurable changes in these frequencies. Moreover, modal behavior provides more detailed information about the damage distribution, especially when frequency changes alone are insufficient to pinpoint the exact

* Corresponding author.
E-mail addresses: m.mashayekhi@kntu.ac.ir (M. Mashayekhi).

https://doi.org/ 10.22080/ceas.2025.29333.1016
ISSN: 3092-7749/
How to cite this article: Alavi, S. H., Pilehvaran, A., Mashayekhi, M. Damage Identification in Truss Structures Using a Hybrid PSO-HHO Algorithm with Selective Natural Frequencies and Mode Shape. Civil Engineering and Applied Solutions. 2025; 1(2): 55–73. doi:10.22080/ceas.2025.29333.1016.

location of the damage [12,13]. Extensive research has been conducted to detect structural damage using various indicators derived from dynamic characteristics [14–18]. Among these indicators are methods based on modal data correlation, parameter estimation techniques [19], frequency response functions [20], and geometric transfer matrices [21].

Non-destructive damage identification methods in structures are typically formulated as inverse problems and addressed through two main approaches: closed-form (analytical) solutions and optimization techniques. The closed-form solutions, which rely on precise mathematical relationships, are suitable for simple structures and noise-free data [22]. However, for complex structures or data contaminated with noise, optimization methods are preferred due to their flexibility and ability to handle uncertainties [23,24]. The general approach of optimization methods involves minimizing the discrepancy between the actual structural response and the response predicted by the optimization model. Sahu and Maity [25] investigated the impact of damage on the static behavior of structures using a neuro-genetic algorithm. In various studies, different optimization algorithms have been employed together with modal analyses of structures for damage identification [26–28]. Kaveh and Zolghadr [9] investigated and evaluated the damage present in truss structures under both two-dimensional and three-dimensional conditions using a population-based algorithm.

In this study, a hybrid metaheuristic algorithm is proposed for damage identification in truss structures using an inverse optimization approach. The objective function is designed to compare the dynamic characteristics of the intact (undamaged) structure with those of the structure under various damage scenarios. Initially, the dynamic characteristics of the intact structure are obtained through structural analysis. Then, by reducing the stiffness in certain truss members, possible damage scenarios are simulated. For each scenario, the dynamic response is computed, and the objective function quantifies the discrepancy between the dynamic characteristics such as natural frequencies and mode shapes of the intact and damaged structures. The metaheuristic optimization algorithm iteratively searches for the damage scenario that minimizes this discrepancy, effectively identifying the most probable location and extent of the damage. This method enables an efficient and automated damage identification process without the need for direct damage measurements, relying solely on changes in the dynamic behavior of the structure. The remainder of the paper is organized as follows: Section 2 presents the damage identification formulation. Section 3 describes the proposed metaheuristic algorithm. Section 4, presented the optimization formulation of this study. Section 5, described the methodology of damage detection with hybrid optimization algorithms. Section 6 presents a structural case study to evaluate the efficiency of the proposed method. Section 7 discusses the results of the case study, in Section 8 discusses the limitation of this study, and finally, Section 9 provides the conclusions of the research.

2. Modal-based damage identification in truss structures

In the term of structural health monitoring, damage identification is modeled as an optimization problem aimed at detecting changes in dynamics structural parameters such as natural frequencies, mode shape, particularly reductions in member stiffness. These changes lead to observable variations in dynamic properties such as natural frequencies and mode shapes. In this section, a concise formulation for structural damage identification based on changes in natural frequencies is presented. The analysis process begins with a review of the displacement-based finite element equations.

2.1. Structural dynamic equation

The dynamic equation of motion for an undamped multi-degree-of-freedom system is expressed in Eq. 1:

$$[M]\{\ddot{x}\} + [K]\{x\} = 0 \tag{1}$$

where *K* is the stiffness matrix and *M* is the mass matrix, while *x* is the displacement vector corresponding to the dynamic problem. For clarity in expressing the finite element terms, a truss structure composed of *n* elements is considered as the system in this study. In finite element modeling of truss structures, each member is idealized as a two-node bar element that is subjected only to axial forces. This method follows a displacement-based approach, in which the overall structural response is assembled from the behavior of individual elements. Accordingly, the equations corresponding to the dynamic characteristics of the truss structure are presented in following. For a bar element with length *L*, cross-sectional area *A*, and Young's modulus *E*, the stiffness matrix in the local coordinate system is defined by Eq. 2 [29].

$$[k_e] = \frac{AE}{L}\begin{bmatrix} 1 & -1 \\ -1 & 1 \end{bmatrix} \tag{2}$$

Assuming a uniform mass distribution along the member, the mass matrix in the local coordinate system is defined as shown in Eq. 3.

$$[m_e] = \frac{\rho AL}{6}\begin{bmatrix} 2 & 1 \\ 1 & 2 \end{bmatrix} \tag{3}$$

For an element in a two-dimensional structure, the structural properties are transformed from the local coordinate system to the global coordinate system using the transformation matrix *T*, as defined in the Eq. 4.

$$[T] = \begin{bmatrix} C & S & 0 & 0 \\ -S & C & 0 & 0 \\ 0 & 0 & C & S \\ 0 & 0 & -S & C \end{bmatrix} \tag{4}$$

where *C* and *S* represent *cosα* and *sinα*, respectively. The transformed stiffness and mass matrices in the global coordinate system are then obtained through Equations 5 and 6, respectively.

$$[K] = [T]^T.[k_e].[T] \tag{5}$$

$$[M] = [T]^T.[m_e].[T] \tag{6}$$

2.2. Damage formulation

The modal properties of the undamaged structure are obtained by solving the eigenvalue problem. The Eq. 7 is formulated based on the dynamic model of the structure in its free-vibration state, without incorporating any damage.

$$[K]\{\varphi_i\} - \omega_i{}^2[M]\{\varphi_i\} = \{0\} \tag{7}$$

where ω_i denotes the *i*th natural frequency, and ϕ_i represents the corresponding mode shape. These parameters characterize the undamaged modal properties of the structure.

Within the concept of inverse problem-based damage identification, each structural member is typically assigned a damage index that reflects its health condition and quantifies the potential stiffness reduction due to damage. This index, typically denoted by α_i, takes a value between zero and one, where zero indicates a completely healthy member and one corresponds to a fully damaged member. In this study, the stiffness matrix is modified to account for the effect of damaged members and is reformulated accordingly, as presented in Eq. 8

$$[K^d] = \sum_{i=1}^{Ele}(1-\alpha_i).[K_i] \tag{8}$$

To incorporate structural damage, the global stiffness matrix *K* is replaced by a modified stiffness matrix K^d (see Eq. 9), which reflects the stiffness reduction caused by damage. It is assumed that the mass matrix *M* remains unaffected by the damage [30].

$$[K^d]\{\varphi_j^d\} - \omega_j^{d\,2}[M]\{\varphi_j^d\} = \{0\} \tag{9}$$

where ω_j and ϕ_j correspond to the *j*th natural frequency and its associated mode shape of the damaged structure. This eigenvalue equation determines the natural frequencies and mode shapes of the damaged structure, which are utilized in the damage identification process. The process of frequency and mode shape variation due to damage is illustrated schematically in the Fig. 1.

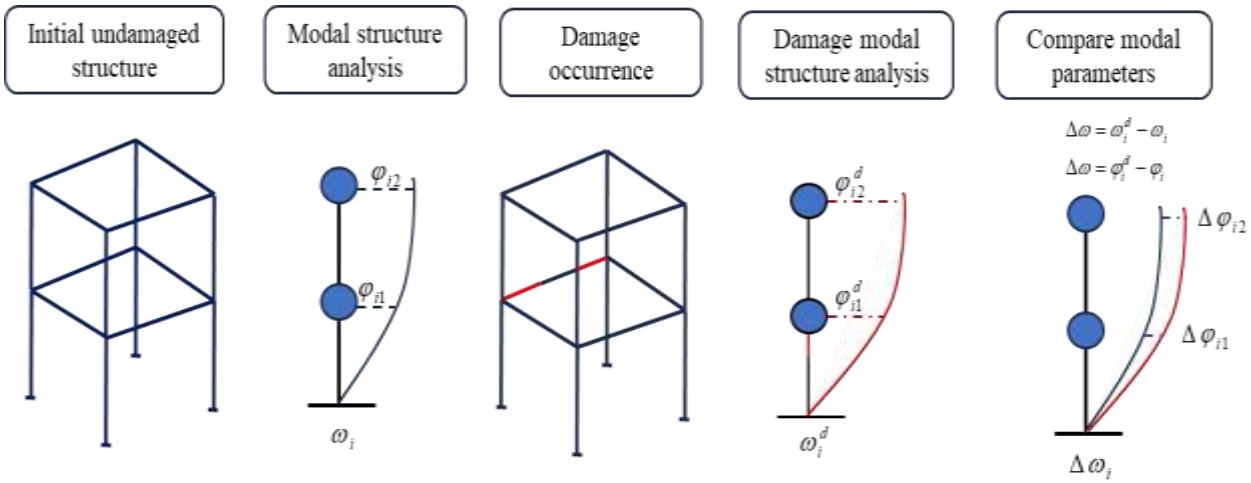

Fig. 1. Schematic representation of frequency and mode shape variations due to structural damage.

3. Optimization approach

In structural damage identification through inverse problem solving, the objective function is typically formulated based on the difference between the observed structural responses and those predicted by the model [31]. This approach typically presents a complex landscape with numerous local minima and multiple global optimal solutions [32]. Therefore, an effective solution to this inverse problem necessitates the use of a robust optimization algorithm capable of thoroughly and efficiently exploring the search space to accurately identify the most probable damage configuration. In recent years, metaheuristic algorithms have been widely employed for structural damage identification [33–35]. Inspired by natural phenomena such as evolution, swarm behavior, or physical laws, these algorithms exhibit strong global search capabilities and are less susceptible to the challenges posed by the non-convex nature of the objective function. Their ability to effectively handle discrete or continuous variables, noisy data, and complex search spaces makes metaheuristic algorithms particularly well-suited for solving inverse problems related to structural damage identification [36]. In this study, a hybrid metaheuristic algorithm combining particle swarm optimization and the harris hawks

optimization algorithm is proposed. First, the structures of each base algorithms are reviewed, and subsequently, the hybrid algorithm is presented.

3.1. Particle swarm optimization (PSO) algorithm

The PSO is a population-based metaheuristic algorithm inspired by the social behavior of animals searching for food [37]. In this algorithm, each particle represents a potential solution and navigates through the search space by updating its position based on its own experience and the experience of neighboring particles. Each particle possesses both a position and a velocity, and its movement is influenced by personal experience (its own best previous position) and social experience (the best position found by the entire swarm). In each iteration, the velocity of a particle is updated based on its personal best position and the global best position found by the swarm. Subsequently, the particle's new position is determined [38,39]. Through repeated iterations, the particles gradually converge toward optimal regions of the search space. The general steps of the PSO algorithm can be summarized as follows:

1. Initially, the position and velocity of each particle are randomly initialized within the defined bounds of search space, as expressed in Eq. 10.

$$\begin{aligned} x_i^{(0)} &= x_{min} + r_1.(x_{max} - x_{min}) \\ v_i^{(0)} &= v_{min} + r_2.(v_{max} - v_{min}) \end{aligned} \tag{10}$$

   The variables r_1 and r_2 are uniformly distributed random numbers in the range [0, 1]. The subscripts *min* and *max* denote the lower and upper bounds of the search space for the particle's position *x* and velocity *v*, respectively.

2. The objective function is evaluated for each particle, and both the personal best position and the global best position are updated accordingly.

3. The velocity of each particle is updated based on three components: momentum, the tendency toward its own best-known position (P_i), and the tendency toward the best-known position of the entire swarm (P_G), according to the Eq. 11. Using the updated velocity, the position of each particle is updated according to the following Eq. 12.

$$v_i^{(t+1)} = \omega.v_i^{(t)} + c_1.r_1.(P_i - x_i^{(t)}) + c_2.r_2.(P_G - x_i^{(t)}) \tag{11}$$

$$x_i^{(t+1)} = x_i^{(t)} + v_i^{(t+1)} \tag{12}$$

4. In each iteration, if a particle's current objective function value is better than its personal best, its best-known position is updated accordingly. Similarly, if the P_G improves, it is also updated. This process continues until a stopping criterion is met either reaching the maximum number of iterations or observing no significant improvement in the global best over several consecutive iterations [40]. Further details of the PSO algorithm are presented in [41,42].

3.2. Harris hawks optimization (HHO) algorithm

The HHO algorithm is a bio-inspired metaheuristic approach that draws inspiration from the collaborative hunting tactics of harris' hawks, introduced by Heidari et al. in 2019 [43]. These birds employ adaptive, group-based strategies that respond dynamically to prey movements and environmental factors. The HHO replicates these behaviors through an iterative process that effectively balances global exploration with local exploitation using probabilistic and adaptive techniques. By modeling hunting stages such as sudden ambushes and varied besieging maneuvers, the algorithm navigates complex search spaces to identify optimal solutions. Owing to its flexibility, robustness, and ease of implementation, the HHO has been successfully applied to a wide range of optimization problems in engineering and science. The main step of the HHO algorithm described in following.

1. Generate an initial population of *n* hawks, each representing a solution vector in a search space. Each variable is randomly initialized within its bounds, as expressed in Eq. 13:

$$x_i^{(j)} = x_{min}^{(j)} + r.\left(x_{max}^{(j)} - x_{min}^{(j)}\right) \tag{13}$$

   The variables *r* is random number uniformly distributed in the range [0, 1]. The subscripts *min* and *max* denote the lower and upper bounds of the search space for the hawk's position *x*.

2. After initializing the population, the algorithm evaluates each hawk's fitness and selects the best one (with the lowest objective value) as the rabbit (i.e., the current best solution). This best solution guides the movement of the rest of the hawks and is updated whenever a better solution is found during the iterations.

3. The HHO algorithm adjusts its search based on the prey's escape energy, defined by Eq. 14.

$$E = 2E_0\left(1 - \frac{t}{T}\right) \tag{14}$$

where E_0 in range -1 to 1, is the initial energy, t is the current iteration, and T is the maximum iterations. If $|E| \geq 1$, the HHO algorithm explores broadly by using Eq. 15.

$$x_{t+1} = \begin{matrix} x_{rand} - \alpha_1 |x_{rand} - 2\alpha_2 x_t| & q \geq 0.5 \\ x_{rabbit} - \bar{x} - \alpha_3 (lB + \alpha_4 (uB - lB)) & q < 0.5 \end{matrix} \quad (15)$$

where x_{rand} is a randomly selected hawk, $\bar{x}$ is the average position of hawks, and α_i, q are random numbers. In $|E| < 1$, the hawks switch to exploitation with different strategies depending on E a random number α. In this phase, for soft besiege ($|E| \geq 0.5$ and $\alpha \geq 0.5$) and hard besiege ($|E| < 0.5$ and $\alpha \geq 0.5$), using Eqs. 16 and 17, respectively.

$$x_{t+1} = \Delta x - E.|J.x_{rabbit} - x_t|, \Delta x = x_{rabbit} - x_t \quad (16)$$

$$x_{t+1} = x_{rabbit} - E.|\Delta x| \quad (17)$$

4. After reaching the maximum iteration T, return the best solution X_{rabbit} as the optimal result. More detail of the HHO algorithms is expressed in [44].

3.3. Hybrid metaheuristic optimization algorithm PSO-HHO

The hybrid PSO-HHO algorithm integrates the strengths of both methods to address complex optimization problems effectively. The PSO's rapid convergence and robust global search complement HHO's adaptive strategies, which balance exploration and exploitation [45]. This hybridization mitigates PSO's tendency to get trapped in local optima by leveraging HHO's diverse hunting mechanisms [46], such as surprise pounce and Levy flight-based jumps, while enhancing HHO's slower convergence in high-dimensional problems through PSO's collective dynamics. By integrating these features, the hybrid algorithm achieves improved efficiency, stability, and solution quality in multimodal optimization tasks.

The hybrid PSO-HHO algorithm integrates PSO and HHO by dividing the population into two interacting subgroups to optimize complex problems. The PSO subgroup rapidly explores the search space using collective particle dynamics, updating positions based on individual and global best solutions. Meanwhile, the HHO subgroup refines solutions through adaptive hunting strategies, such as surprise pounce and dynamic besieging, focusing on precise exploitation. Interaction occurs iteratively: PSO shares its top-performing solutions with HHO to enhance local search precision, while HHO's best solutions guide PSO's global exploration by updating its reference points [47]. A probabilistic crossover mechanism blends solutions from both subgroups to maintain diversity and prevent premature convergence. This cooperative framework leverages PSO's fast global search to accelerate HHO's slower convergence in high-dimensional spaces. In turn, HHO's adaptive strategies help PSO escape local optima, resulting in improved solution accuracy, robustness, and efficiency for multimodal optimization tasks [48]. The Fig. 2 provides an overview of the hybrid algorithm, illustrating the interactions between PSO and HHO algorithm.

4. Optimization formulation

This section addresses the key aspects of applying the proposed optimization algorithm to structural damage identification. The formulation includes the definition of decision variables, the specification of problem constraints, and the construction of the objective function that are fundamental components of any optimization process. The decision variables in this study are defined as stiffness reduction factors for each structural element, resulting in a total variable count equal to the number of elements in the model. The optimization problem is formulated as an unconstrained problem, with no additional constraints applied to the decision variables or the solution space. The primary objective is to minimize the discrepancy between the dynamic response obtained from the computational model and the response measured from the actual (possibly damaged) structure. This discrepancy is quantitatively represented through an objective function. To this end, the objective function is defined as $f(\alpha)$, which evaluates the difference between the computed and measured modal parameters. This function typically consists of two main components:

1. Frequency difference term: this component evaluates the relative difference between the natural frequencies computed from the numerical model and those measured from the damaged structure, as expressed by the Eq. 18:

$$f_1(\alpha) = \sum_{i=1}^{n_f} \left(\frac{\omega_i^d - \omega_i}{\omega_i}\right) \quad (18)$$

2. Mode shape difference term: this component quantifies the discrepancy between the measured and computed mode shapes as expressed in Eq. 19. Finally, the objective function is computed as a weighted combination of the previously defined components, as expressed in the Eq. 20.

$$f_2(\alpha) = \sum_{i=1}^{n_f} \sum_{j}^{n} \left(\frac{\varphi_{(i,j)}^d - \varphi_{(i,j)}}{\varphi_{(i.j)}}\right) \quad (19)$$

$$f(\alpha) = f_1(\alpha) + f_2(\alpha) \quad (20)$$

3. wehrer n_f and n are representing the number of modes and the number of degrees of freedom, respectively. The objective function is formulated to assess the degree of agreement between the response of the damaged structure and that predicted

by the assumed damage scenario. The aim of the optimization process is to identify the damage scenario that results in the smallest discrepancy from the actual behavior of the damaged structure. A lower objective function value reflects a closer match between the simulated scenario and the true structural response. This process involves repetitive iterations to achieve minimization. The next section introduces the methodology of damage detection based proposed hybrid metaheuristic algorithm used in this study.

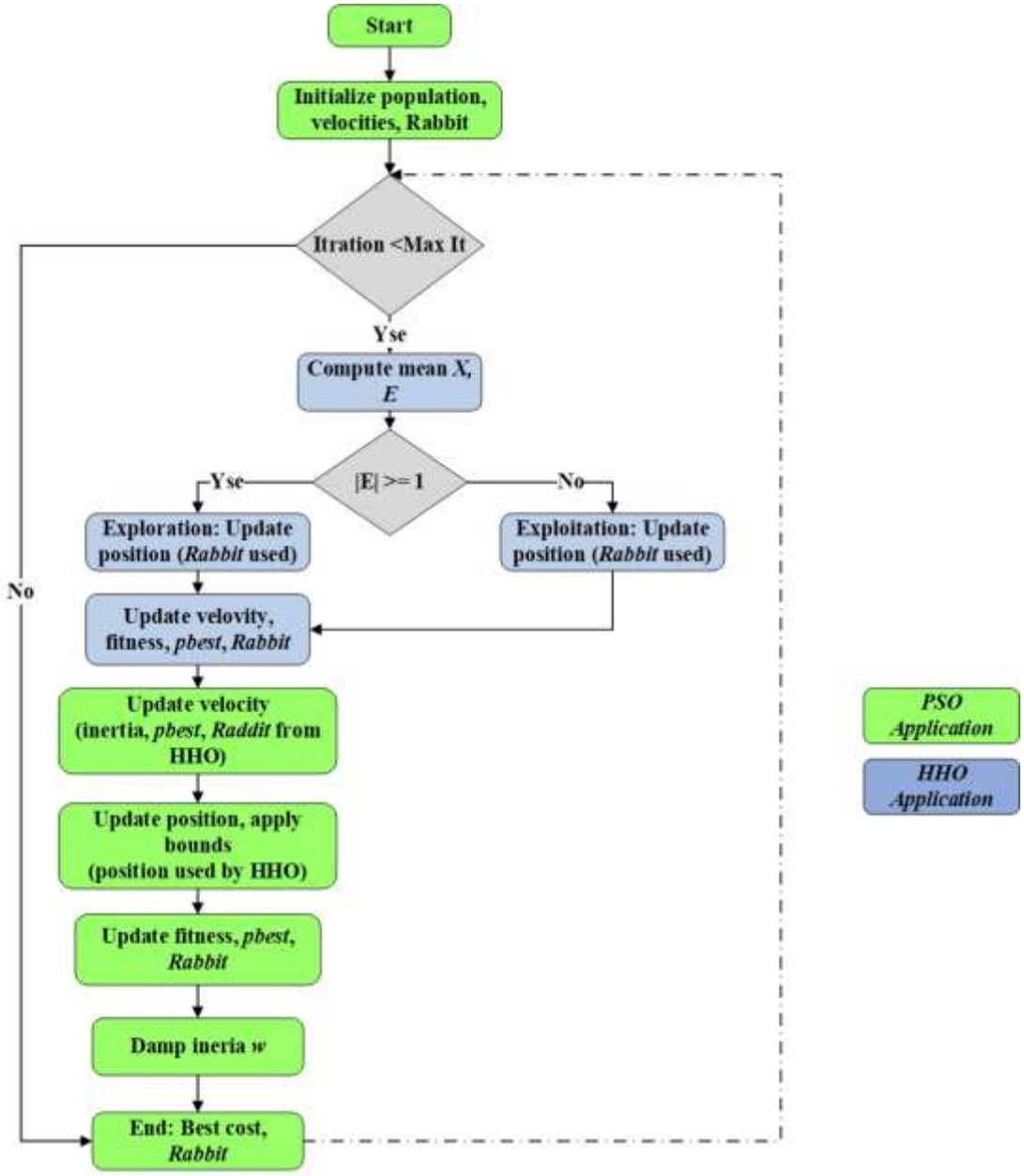

Fig. 2. Flowchart of the hybrid PSO-HHO algorithm.

5. Proposed framework for detecting structural damage

In this research, structural damage is identified and evaluated by leveraging principles related to the dynamic response of the system. Techniques based on vibration analysis rely on the premise that a structure's dynamic characteristics are inherently linked to its physical properties. Alterations in key structural matrices lead to observable variations in natural frequencies and mode shapes. This relationship forms the basis for damage detection, which can be approached by defining an optimization problem. As discussed in the preceding sections, the aim is to reduce the difference between the dynamic behavior represented by the damaged model and that observed in the experimental data, which forms the basis for defining the objective of the analysis.

The initial phase of the proposed approach involves modeling of a finite element model that reflects the intact state of the structure. The damaged structural model is simulated by reducing the stiffness in the basic structural members through the stiffness matrix. In this framework, for second phase, the optimization variables are defined as stiffness reduction coefficients assigned to individual structural elements, with the total number of variables corresponding to the number of elements within the model. The parameters selected for formulating the objective function should exhibit high sensitivity to structural damage. Accordingly, the objective function is formulated based on a combination of the structure's modal properties, namely natural frequencies and mode shapes. In the third phase, the dynamic parameters corresponding to the damaged condition must be obtained experimentally. Each

damage scenario is characterized by a set of affected elements and their associated levels of damage. Choosing and setting up the optimization algorithm is key for effective damage detection. In this study, a hybrid PSO-HHO algorithm is employed to leverage the complementary strengths of both algorithms. The initial population is generated using heuristic strategies to effectively explore the search space, focusing on potential damage scenarios with varying severity. The hybrid algorithm iteratively updates candidate solutions, ultimately selecting the best-performing solution as the damage identification result. The identified damage scenario includes all elements exhibiting damage levels exceeding a predefined threshold, while elements with lower damage values are treated as undamaged. The hybrid PSO-HHO algorithm is executed multiple times, and the solution corresponding to the lowest objective function value is selected as the most representative damage scenario. The step-by-step process of the proposed damage detection methodology presented in this study is illustrated in Fig. 3.

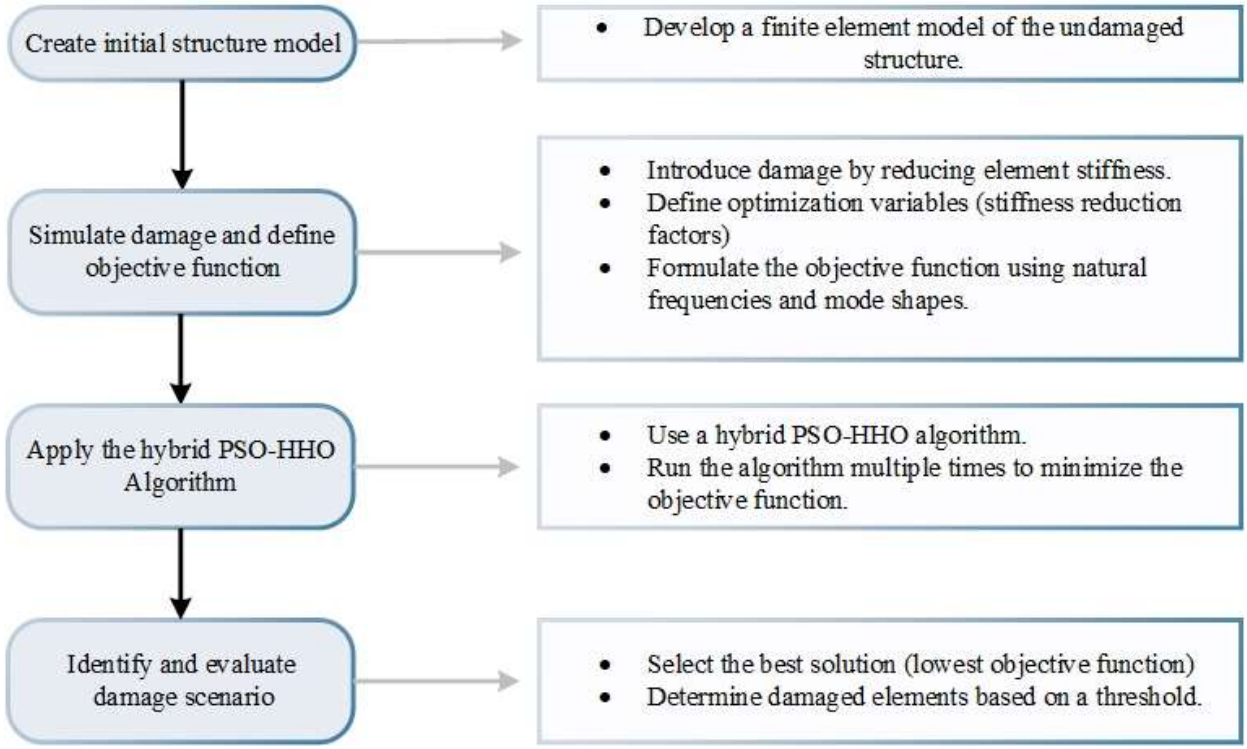

Fig. 3. Flowchart of the proposed damage detection method using a hybrid PSO-HHO algorithm.

6. Proposed examples

This section provides numerical simulations to evaluate the effectiveness of the proposed hybrid PSO-HHO algorithm in identifying structural damage within 2D truss systems. Since the damage identification algorithm is implemented based on the behavior of truss structures, two benchmark truss case studies are considered in this section. The first case involves a 15-element planar truss, as illustrated in Fig. 4, based on the model presented by Laier and Villalba [49]. In terms of degrees of freedom, all nodes except Node 1 and Node 5 have two translational degrees of freedom in the 2D plane. Node 1 is constrained in one direction and therefore retains only a single degree of freedom. In total, the truss system comprises 13 degrees of freedom. Both vertical and horizontal elements have a length of 1 meter.

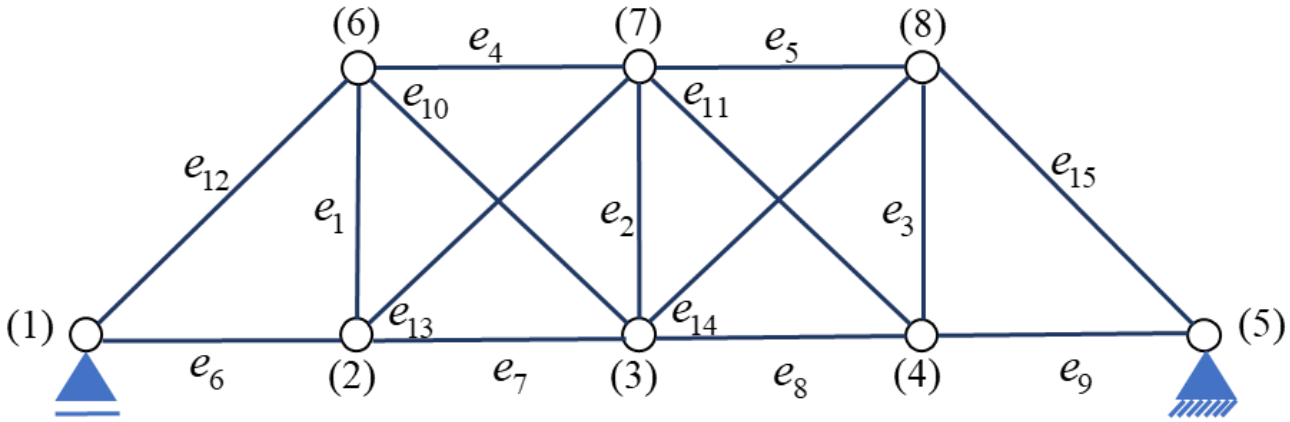

Fig. 4. Schematic of the first case study.

The second case study is an 11-member planar truss structure introduced by Russell Hibbeler, as shown in Fig. 5, with specific constraint [50].

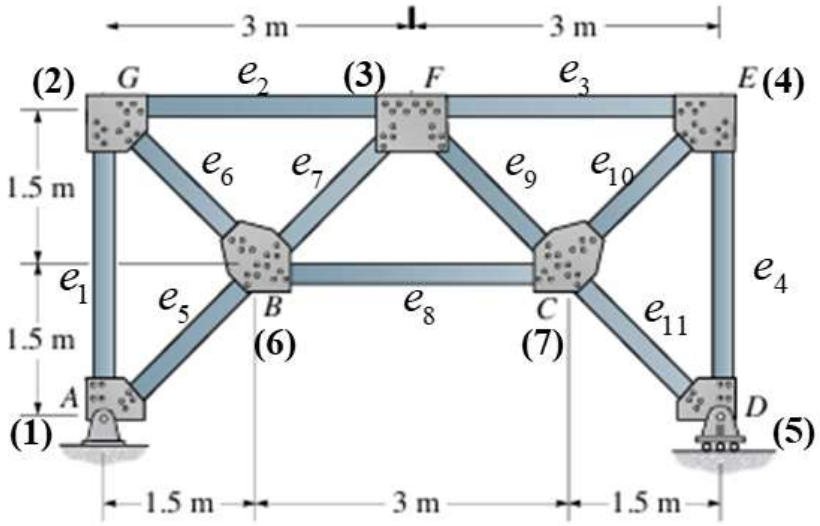

Fig. 5. Schematic of the second case study [50].

In two case study, the structural members are defined with a Young's modulus of E=200 GPa, material density of ρ=7800 kg/m³, and a uniform cross-sectional area of A=0.001 m². For this case study, various damage cases are considered, as summarized in Table 1.

Table 1. Various damage cases considered for the truss.

Case study	Damage scenario	Damaged structural element	damage intensity
First	Scenario 1	13	0.33
	Scenario 2	6, 11	0.2, 0.15
Second	Scenario 1	1	0.55
	Scenario 2	8	0.45
	Scenario 3	6, 11	0.25,0.15

7. Result

This section presents the observations and results related to truss damage identification under various damage scenarios in each truss case study. Generally, the truss structure in each case study is analyzed for 500 iterations with a population size of 300 for both single-element damage and multiple-element damage. The hybrid PSO–HHO algorithm combines the strengths of PSO and HHO to achieve a well-balanced trade-off between exploration and exploitation in complex search spaces. In the PSO component, key parameters such as inertia weight, cognitive coefficient, social coefficient, and velocity limits govern the dynamic behavior of particles. The inertia weight in this study starts at 0.9 and gradually decreases over the course of iterations. The cognitive and social learning coefficients typically range from 1.0 to 2.5, with standard values often set around 2.0. However, in this study, both the cognitive and social coefficients were set to 1.12, based on trials within the conventional range. Higher values led to decreased performance or failure to converge. On the other hand, the HHO component incorporates adaptive mechanisms for diversification through two key parameters: escaping energy and jump strength. The gradual decay of escaping energy across iterations facilitates the transition from global exploration in the early stages to local exploitation in the later stages. This adaptive behavior helps prevent premature convergence and encourages a more comprehensive exploration of the solution space. The escaping energy decreases linearly to enhance diversity and avoid entrapment in local optima. The jump strength, which determines the magnitude of random movement, is governed by randomly generated values. A summary of each parameter and its corresponding value is provided in Table 2. The following section presents the results related to the two case studies. In the first case study, in addition to the initial damage detection results, detailed statistical analyses and the individual performance of each algorithm are provided. Finally, in the second case study, the results of damage identification are presented and discussed.

Table 2. Parameters of the Hybrid PSO-HHO Algorithm.

Parameter	Description	Value or Range
w	Inertia weight controlling the influence of the previous velocity on the current one (*PSO*)	0.9
c_1	Cognitive acceleration coefficient; determines the impact of the particle's own best experience on its velocity (*PSO*)	1.12
c_2	Social acceleration coefficient; determines the influence of the global best position (rabbit) on the particle's movement (*PSO*)	1.12
Maximum velocity	Maximum velocity allowed for particles; used to limit how far a particle can move in a single iteration (*PSO*)	0.2*(upper bound-lower bound)
Minimum velocity	Minimum velocity allowed for particles; ensures that the movement doesn't become too small to be effective (*PSO)*	-upper bound

Escaping energy	Dynamic parameter in HHO controlling the transition between exploration and exploitation; decreases with each iteration (*HHO*)	$2*(1-\frac{it}{max\_it})$ * unifran (-1,1)
Jump strength	Controls the intensity of the Lévy flight-based jumps in HHO; adds randomness to enhance search diversification (*HHO*)	2*(1-rand ())

it: current iteration, *max_it:* maximum iteration
unifrand (-1,1): a random number from a uniform distribution in the range between -1 and 1.

7.1. First case study

The results of damage detection using the proposed hybrid PSO-HHO algorithm are presented in the next. Fig. 6 shows the convergence behavior of the hybrid algorithm across different runs for scenario 1. It is evident that from iteration 100 onwards, the algorithm achieves faster and more accurate convergence. The Table 3 summarizes three key performance indicators mean, initial rate of decrease, and stability for each of the four runs. The initial rate of decrease quantifies the early convergence behavior, measured by the drop in values between the first and second iterations. Stability is assessed by the standard deviation over the final 20% of the iterations, indicating the solution's consistency in the latter stages of the run; lower values correspond to higher stability.

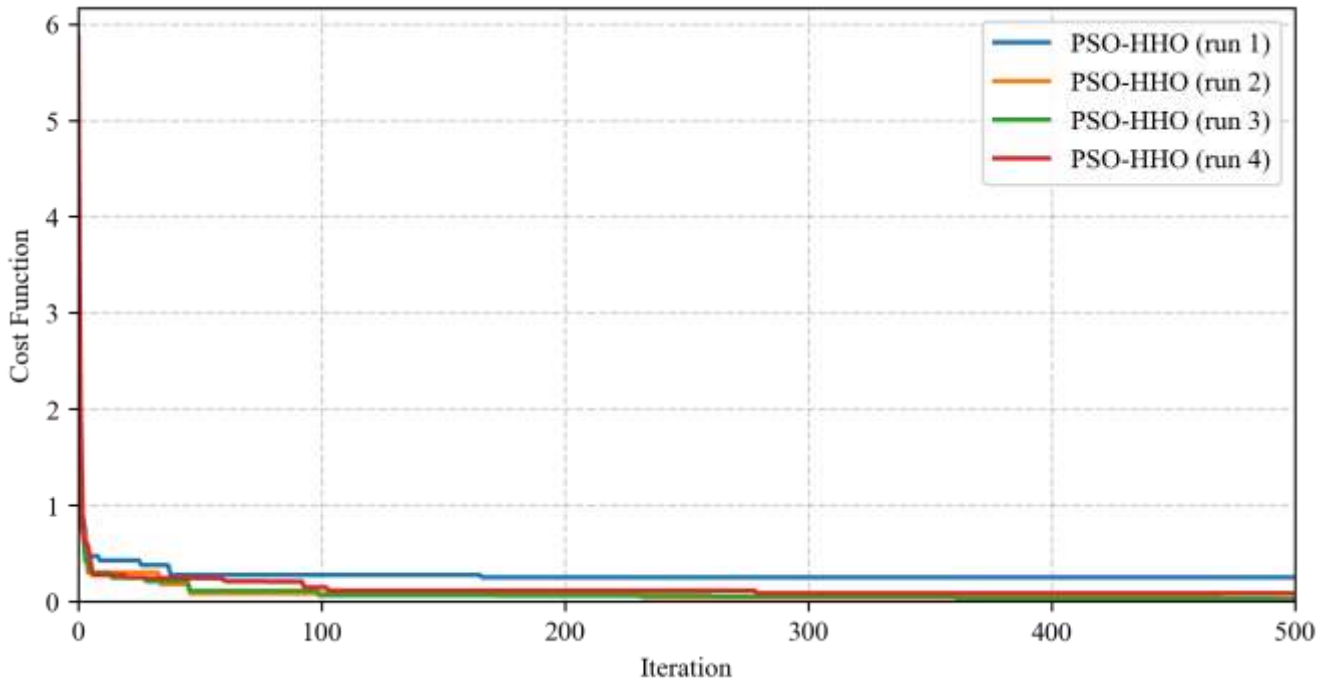

Fig. 6. The cost function of each hybrid PSO-HHO algorithm run for scenario 1.

Table 3. Comparison of performance metrics across four independent runs of the hybrid algorithm for scenario 1.

Run	1	2	3	4
Mean	0.282	0.089	0.083	0.14
Initial rate of decrease	4.25	3.36	2.91	3.78
stability	0.00	0.004	0.0015	0.00

Fig. 7 presents the predicted damage values for scenario 1 in each run of the hybrid algorithm, compared to the actual damage values.

For comparison and to assess the efficiency of the hybrid algorithm, the performance of the individual HHO and PSO algorithms is also described under identical population size and iteration settings. For each algorithm, four independent runs are performed, and the comparison is based on the average results obtained from these runs. Figs. 8 and 9 illustrate the comparison between the hybrid algorithm and the HHO and PSO algorithm, respectively. As shown, the hybrid algorithm significantly outperforms the HHO algorithm. While the performance of the HHO algorithm improves with increasing population size (from 600 to 1000) at a constant number of iterations, a substantial performance gap between the two algorithms remains. However, the population size appears to have had a negligible impact on the performance of the PSO algorithm in this case study, as similar trends were observed across different population settings.

Fig. 10 presents the distribution of the objective function values for the hybrid algorithm alongside the individual algorithms. Compared to Fig. 10a, Fig. 10b demonstrates a more consistent interquartile distribution across the algorithms, indicating a more stable performance of the HHO algorithm relative to PSO. The presence of numerous outliers in the PSO results also suggests a need for further tuning of the standalone PSO algorithm.

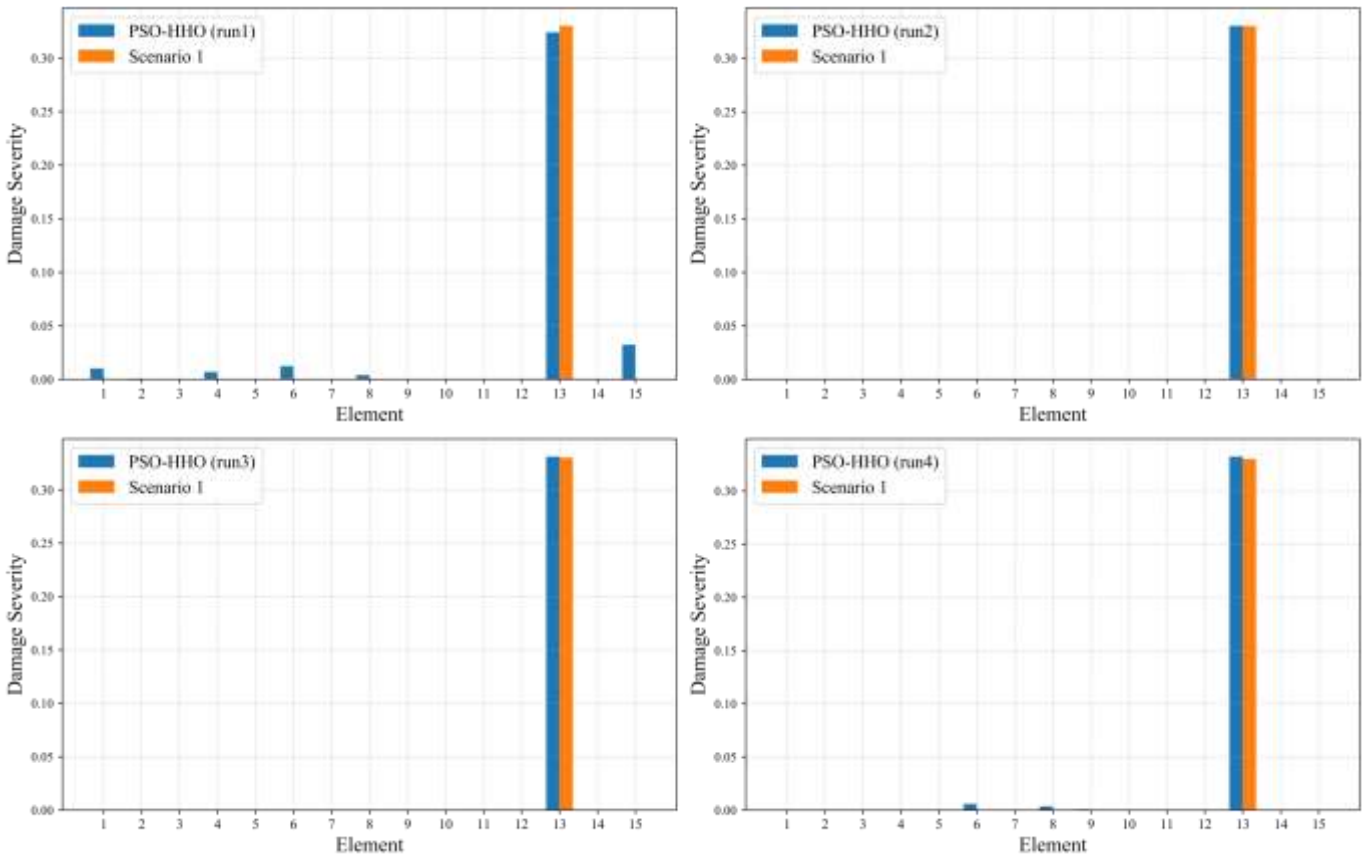

Fig. 7. The damage detection of each hybrid PSO-HHO algorithm run for scenario 1.

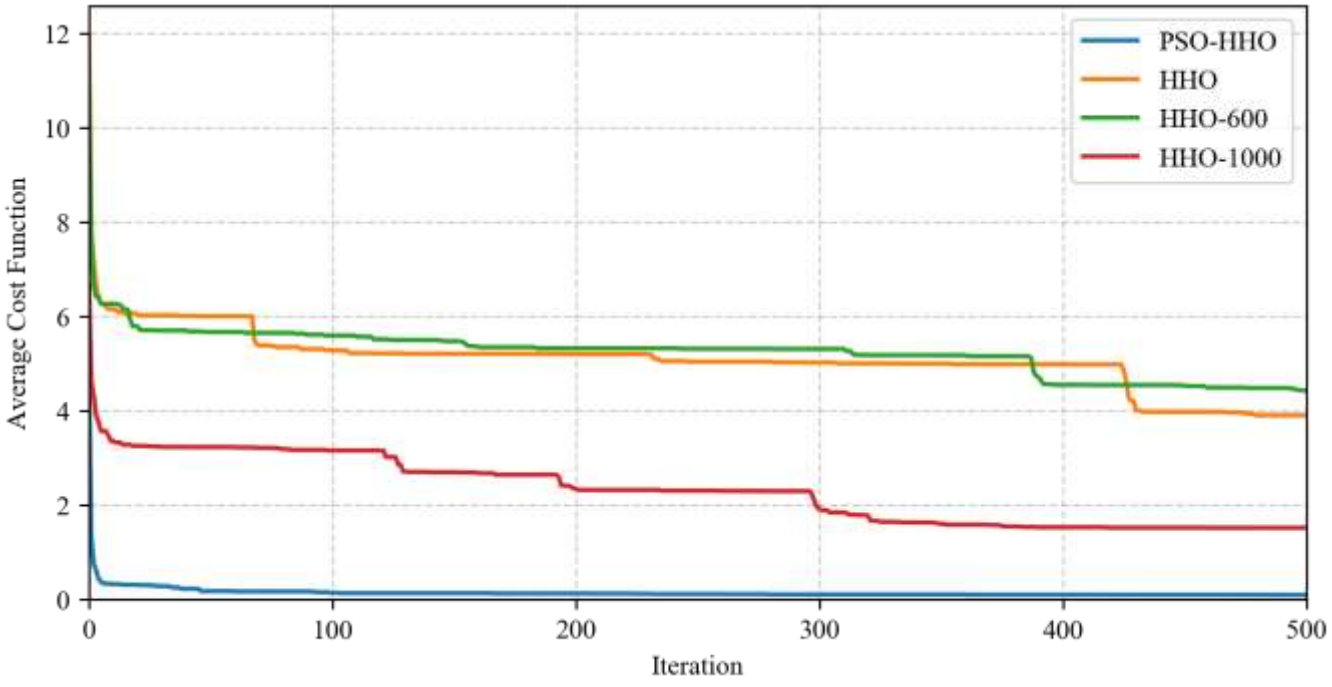

Fig. 8. The performance comparison of hybrid PSO-HHO and HHO for scenario 1.

In addition, statistical indicators provide valuable insight into the performance of each algorithm. Table 4 summarizes the statistical metrics computed for the objective function values obtained from the algorithms. It is worth noting that, for the hybrid algorithm, one of the four conducted analyses has been selected for representation. The PSO-600 algorithm shows the highest mean cost function, while PSO-HHO has the lowest, indicating much better optimization performance. PSO-HHO also exhibits the smallest standard deviation, indicating high consistency across runs. Among the standalone methods, PSO-1000 and HHO-1000 outperformed both their base versions and those with a population size of 600. Overall, the hybrid PSO-HHO approach clearly outperforms both individual PSO and HHO variants in both accuracy and stability.

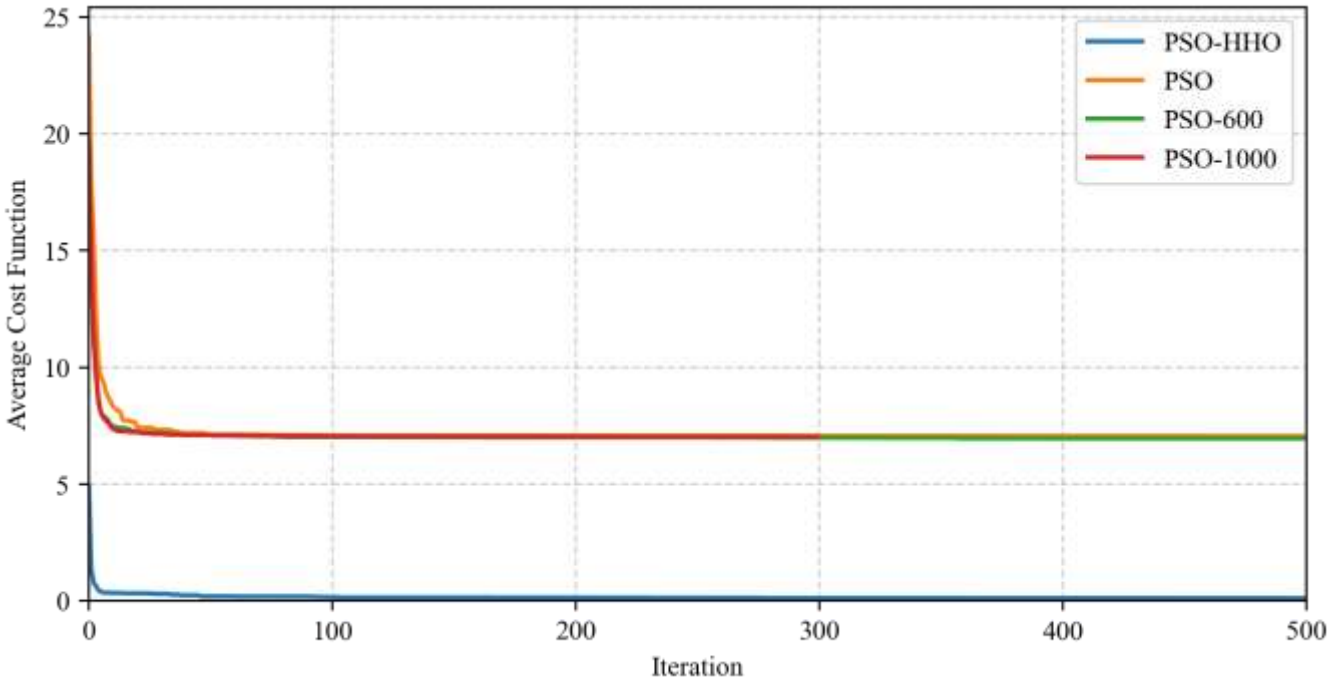

Fig. 9. The performance comparison of hybrid PSO-HHO and PSO for scenario 1.

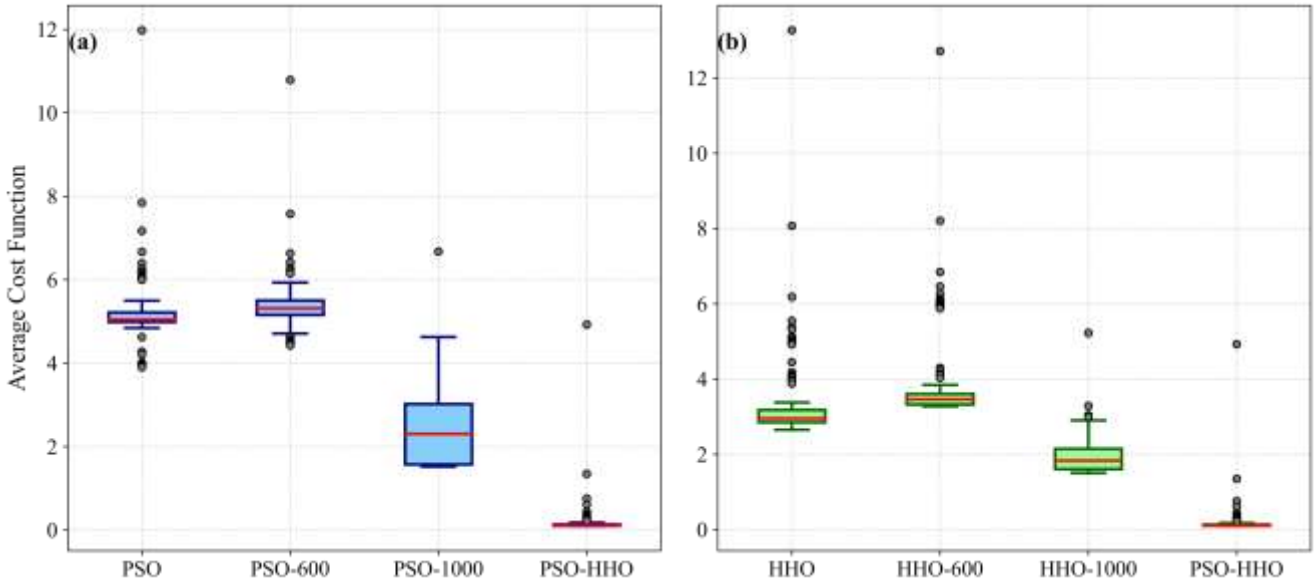

Fig. 10. Evaluation of cost function distributions for PSO, HHO, and hybrid algorithms in scenario 1. a) PSO comparison, b) HHO comparison.

Table 4. Statistical analysis of scenario 1 results for the hybrid algorithm and the individual PSO and HHO algorithms.

item	Mean	STD	Median	Min	Max
PSO	5.09	0.66	5.04	3.90	11.98
PSO-600	5.24	0.51	5.31	4.42	10.79
PSO-1000	2.31	0.70	2.30	1.52	6.68
HHO	3.20	0.78	2.95	2.65	13.27
HHO-600	3.82	0.96	3.46	3.27	12.72
HHO-1000	1.91	0.36	1.83	1.51	5.23
PSO-HHO	0.14	0.22	0.11	0.09	4.92

Fig. 11 shows the convergence behavior of the hybrid algorithm across different runs for scenario 2. Run 1 demonstrating the fastest initial descent and lowest final values, indicating superior performance. The Table 5 summarizes the key performance metrics for each of the four runs in scenario 2. The Run 2 demonstrates the greatest stability with a standard deviation of 0.002 in the last 20% of the data, whereas Run 1 shows the highest variability with a stability of 0.0135 in the same part.

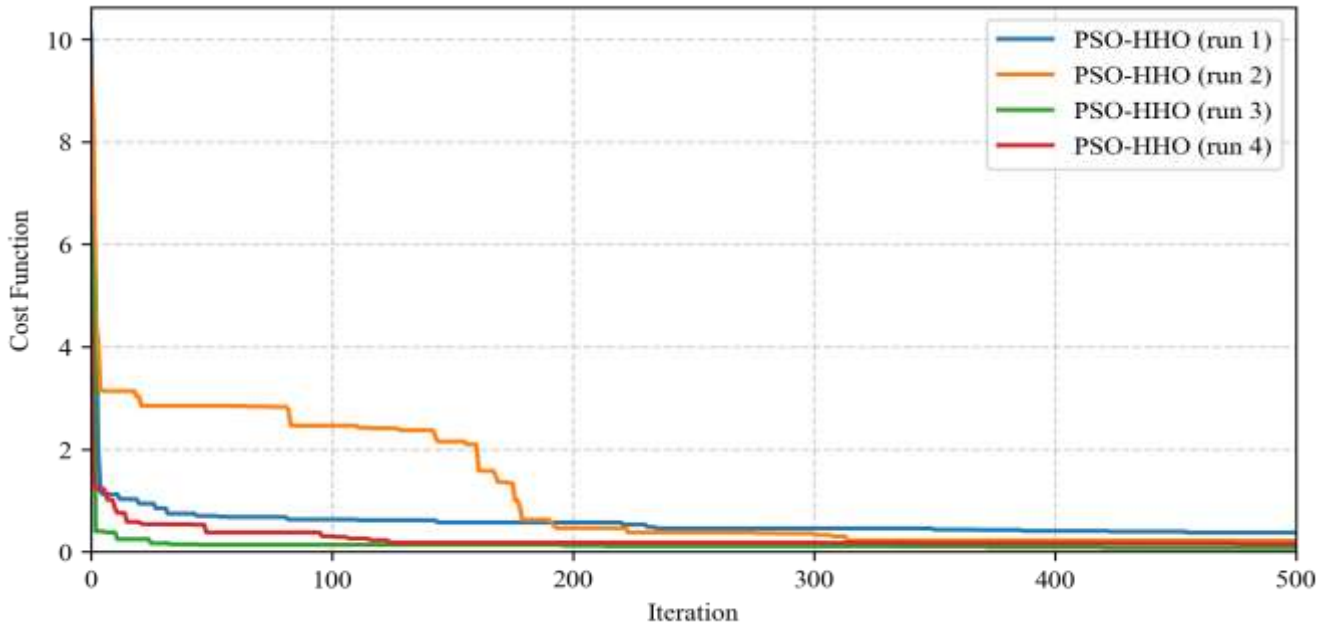

Fig. 11. The cost function of each hybrid PSO-HHO algorithm run for scenario 2.

Table 5. Comparison of performance metrics across four independent runs of the hybrid algorithm for scenario 2.

Run	1	2	3	4
Mean	0.58	1.1	0.14	0.25
Initial rate of decrease	2.37	1.063	1.47	3.17
stability	0.013	0.002	0.006	0.005

Fig. 12 presents the identified damage values for scenario 2 in each run of the hybrid algorithm, compared to the actual damage values. While the algorithm qualitatively demonstrates good performance in damage identification, quantitatively, the estimations occasionally overestimate or underestimate the actual damage values.

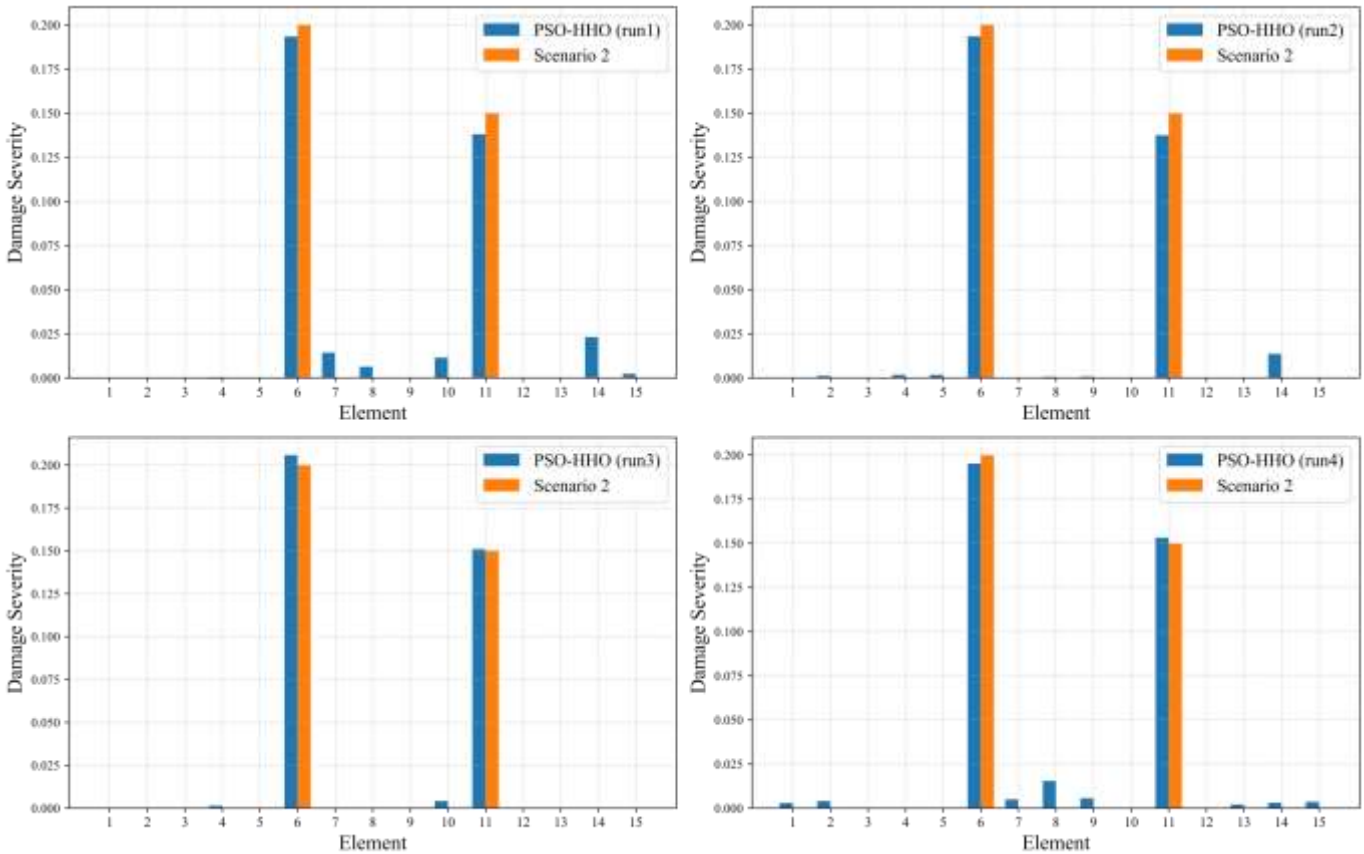

Fig. 12. The damage detection of each hybrid PSO-HHO algorithm run for scenario 2.

Figs.13 and 14 illustrate the comparison between the hybrid algorithm and the HHO and PSO algorithm, respectively. As

observed in scenario 1, the HHO algorithm once again demonstrates inferior performance when compared to the hybrid PSO-HHO algorithm under the same population size. Although HHO improves with larger populations, the hybrid algorithm consistently outperforms it across all settings. The cost function of the hybrid algorithm outperforms the HHO algorithm by approximately 30% to 65%, demonstrating a significantly improved performance. In contrast to scenario 1, increasing the population size has had a moderate impact on the performance of the PSO algorithm; nevertheless, a similar overall trend remains evident across different population sizes.

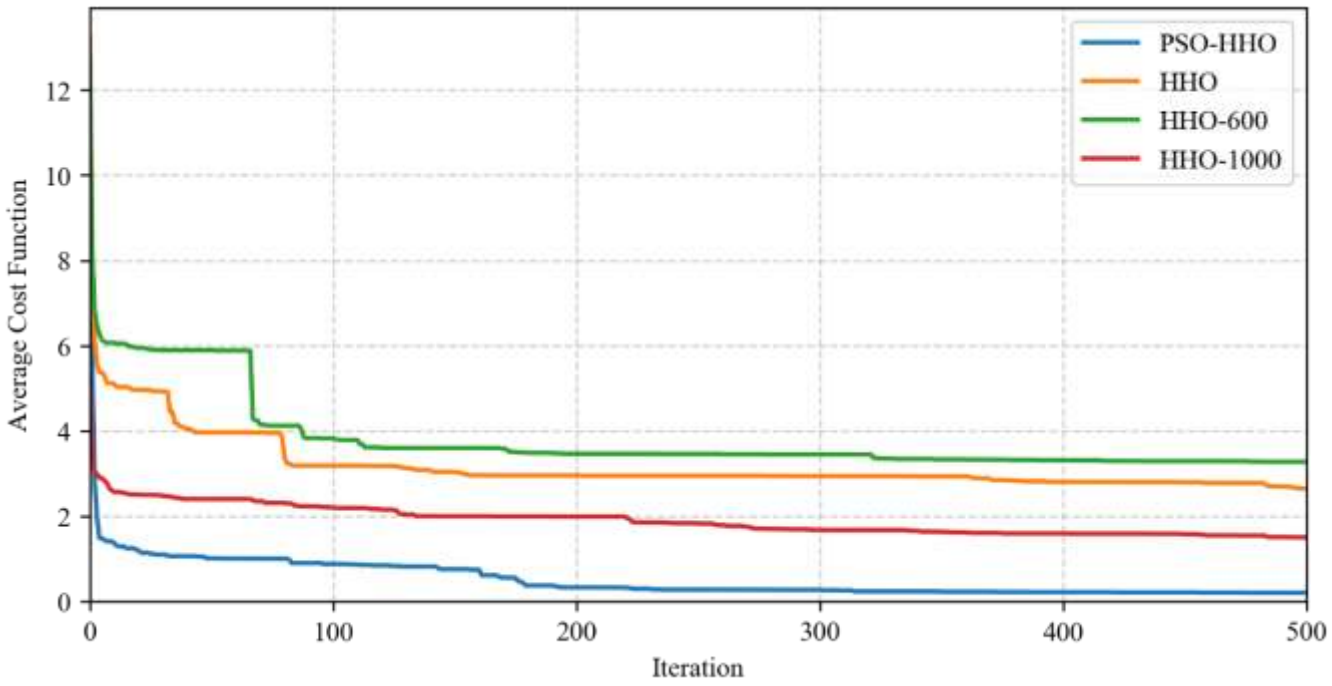

Fig. 13. The performance comparison of hybrid PSO-HHO and HHO for scenario 2.

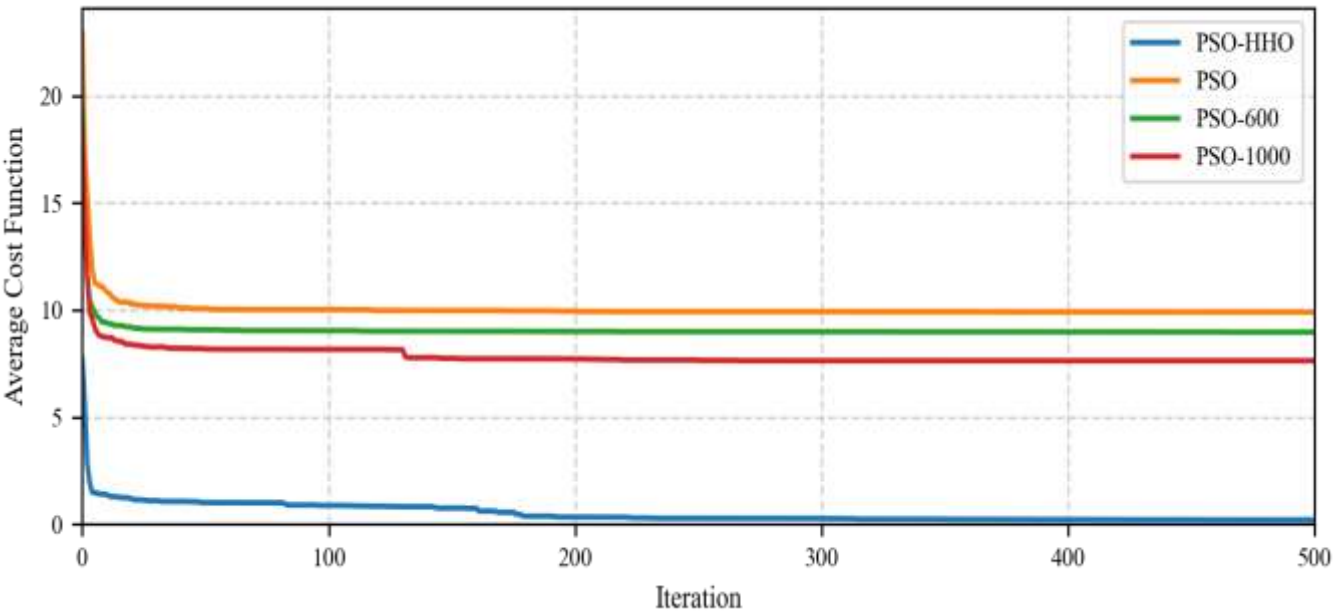

Fig. 14. The performance comparison of hybrid PSO-HHO and PSO for scenario 2.

The distribution and spread of the estimated objective function in this scenario for each algorithm are illustrated in the Fig. 15.

Table 6 presents the statistical parameters related to the objective function values obtained from each algorithm in scenario 2. A review and comparison of these parameters clearly indicate that the hybrid algorithm demonstrates relatively superior performance compared to the individual application of each algorithm in the given example.

7.2. Second case study

In this case study, three different damage scenarios are applied to the truss structure illustrated in Fig. 5. The following section presents the damage detection results obtained by the hybrid algorithm across four independent runs. It is worth noting that, due to the influence of various parameters affecting the performance of the hybrid algorithm, a larger number of analyses is required to reduce uncertainty and achieve stable and reliable results.

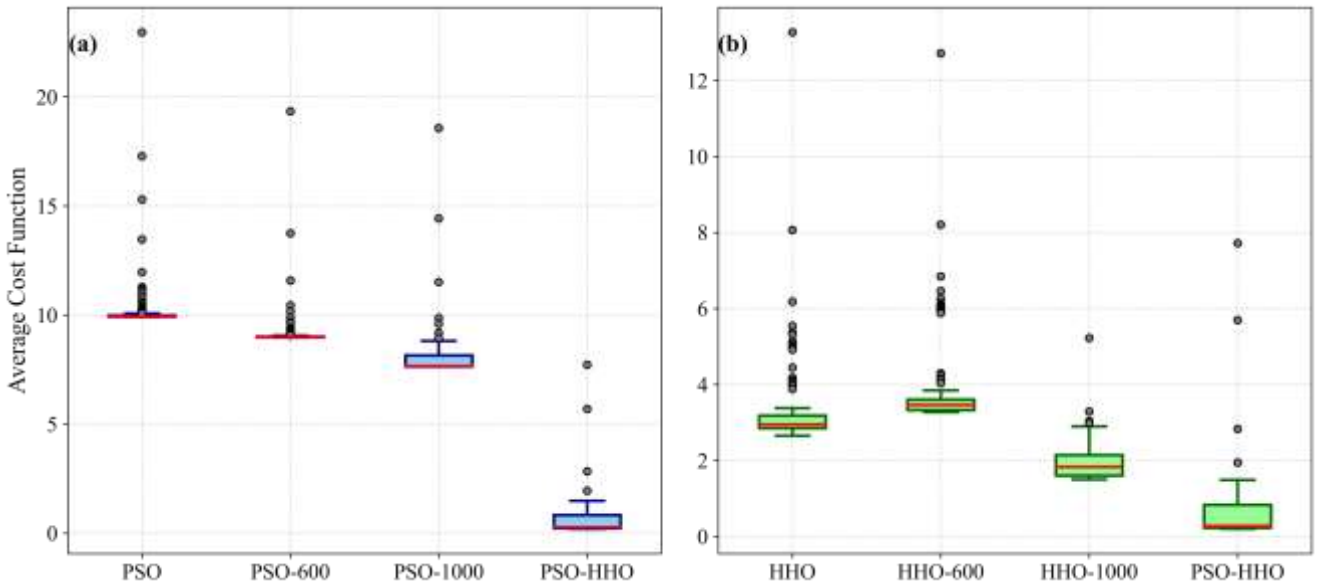

Fig. 15. Evaluation of cost function distributions for PSO, HHO, and hybrid algorithms in scenario 2. a) PSO comparison, b) HHO comparison.

Table 6. Statistical analysis of scenario 2 results for the hybrid algorithm and the individual PSO and HHO algorithms.

item	Mean	STD	Median	Min	Max
PSO	10.04	0.74	9.93	9.91	22.96
PSO-600	9.06	0.53	8.99	8.97	19.33
PSO-1000	7.86	0.65	7.66	7.63	18.56
HHO	3.2	0.78	2.95	2.65	13.26
HHO-600	3.82	0.96	3.46	3.27	12.71
HHO-1000	1.90	0.36	1.83	1.50	5.22
PSO-HHO	0.52	0.54	0.28	0.20	7.72

It is worth noting that, due to the influence of various parameters affecting the performance of the hybrid algorithm, a larger number of analyses is required to reduce uncertainty and achieve stable and reliable results. As illustrated in Fig. 16 the hybrid algorithm has successfully identified the damage located in a single member of the truss structure.

However, in the second scenario (see Fig. 17), although there is also damage in one member, due to its location near the center of the structure, the hybrid algorithm exhibited less stability in damage identification compared to the first scenario. While it successfully detected the damage in the affected member, it also incorrectly reported damage in other members.

Finally, in the third scenario, where two members are damaged, the hybrid algorithm performed qualitatively well by correctly identifying the damaged locations (see Fig. 18). However, from a quantitative perspective, it sometimes underestimates or overestimates the damage severity, which represents one of the algorithm's limitations at this stage. Additionally, the hybrid algorithm estimated minor damage in some other members, which, although small in magnitude, negatively affects the overall stability. The following section discusses some of the reasons behind these limitations.

8. Limitations of study

Although the proposed PSO-HHO algorithm demonstrates high accuracy in identifying damage scenarios under various conditions, it is important to acknowledge its potential limitations. One such limitation arises in cases involving multiple-damage locations that are close to each other or occur in structurally symmetric positions. In these situations, the algorithm may misinterpret the dynamic response, leading to overestimation or underestimation of the damage severity or even misidentification of the damage location. Furthermore, in cases where the modal information is incomplete, highly sensitive to noise, or affected by closely spaced modes, the performance of the hybrid optimization approach may degrade. This is particularly true when measurement errors or modeling inaccuracies are present, which can skew the objective function landscape and cause the algorithm to converge to suboptimal solutions. In addition, it has been observed that in complex scenarios especially those involving multiple damage scenarios the algorithm may require a larger number of iterations or independent runs to achieve consistent and accurate results. This is due to the increased complexity and multimodality of the search space in such cases, which can trap the algorithm in local optima if the search process is prematurely terminated. Therefore, increasing the population size, adjusting the convergence criteria, or applying ensemble or restart strategies may help to enhance performance in these challenging settings.

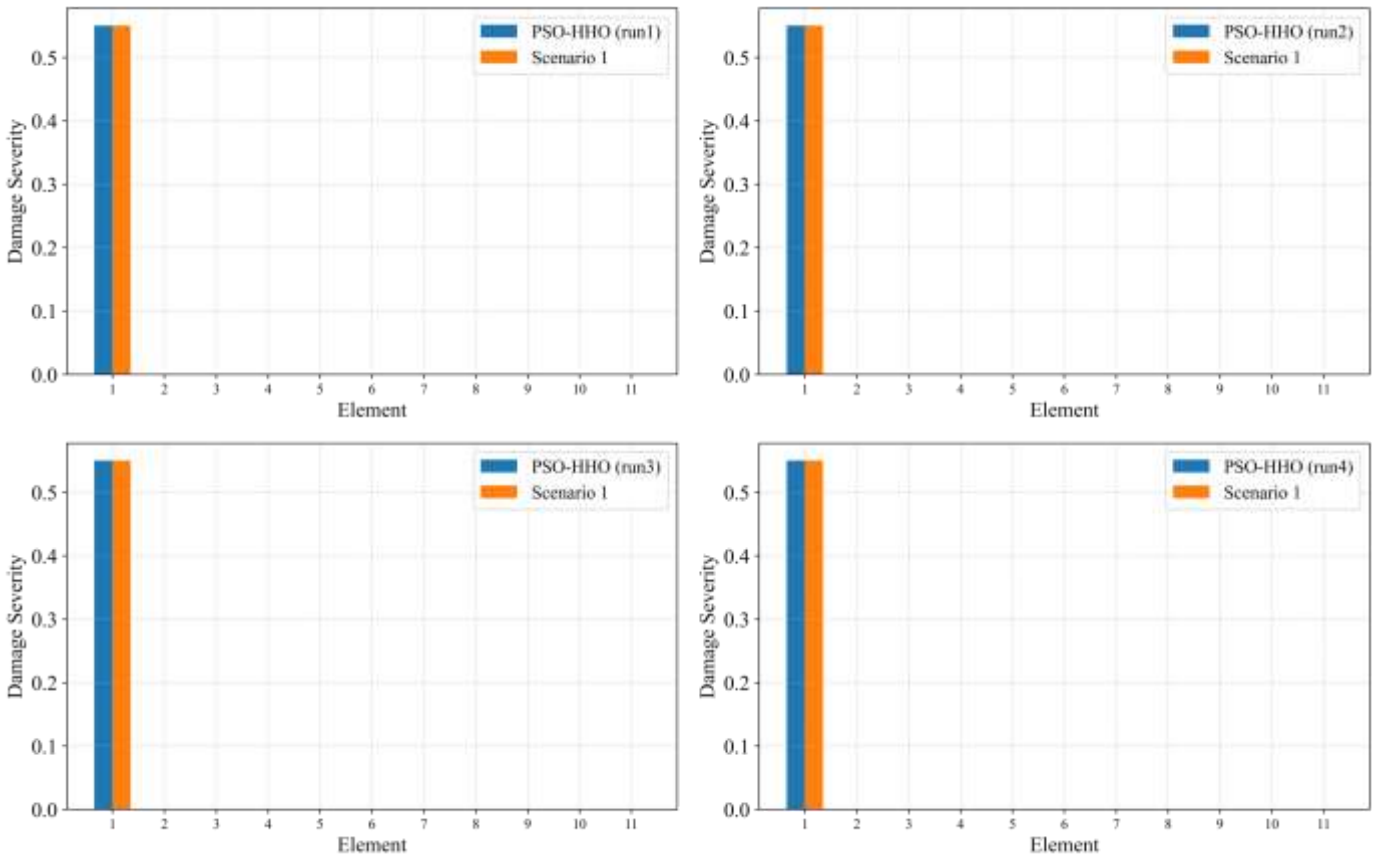

Fig. 16. The damage detection of each hybrid PSO-HHO algorithm run for scenario 1.

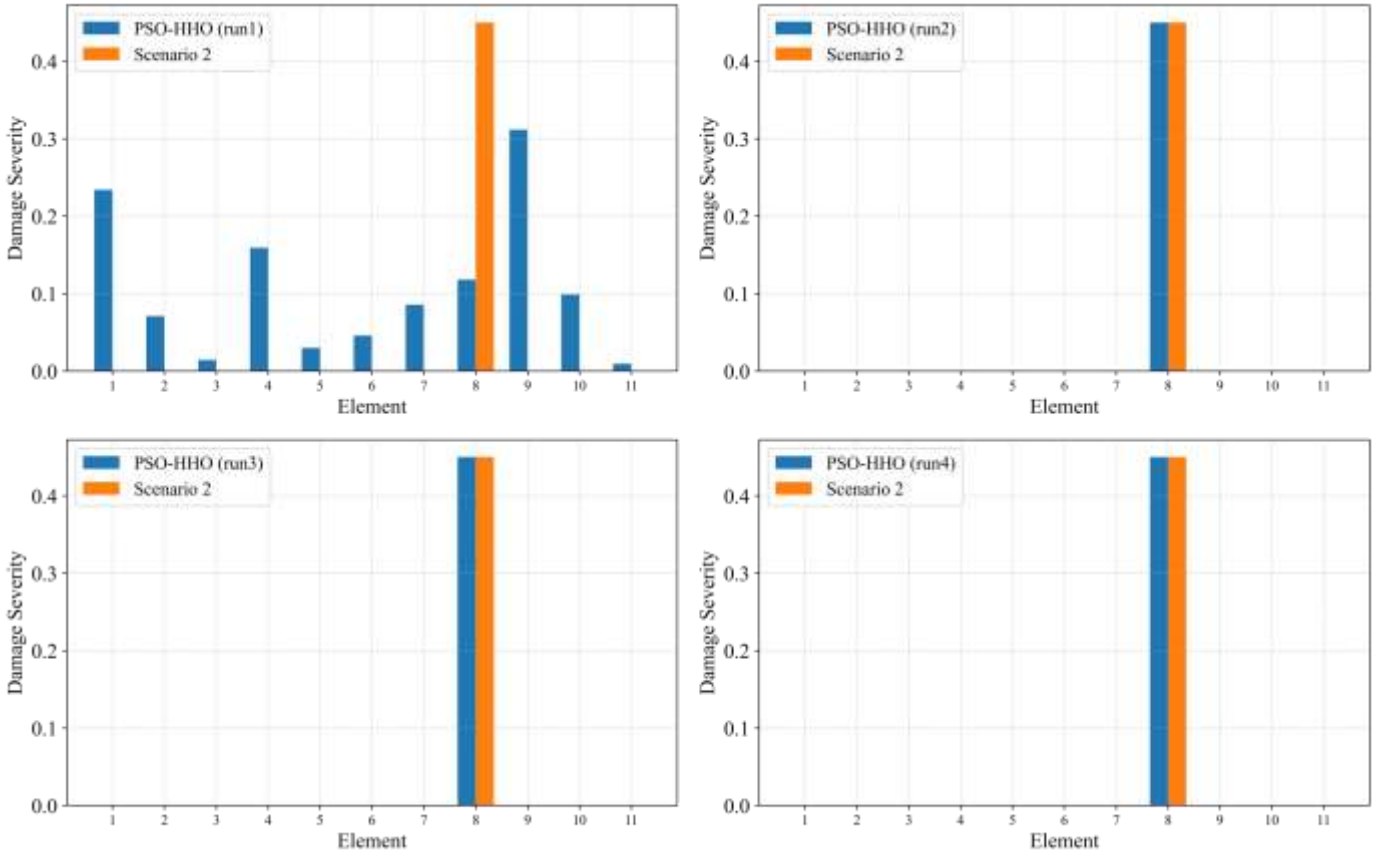

Fig. 17. The damage detection of each hybrid PSO-HHO algorithm run for scenario 2.

These challenges highlight the need for further studies to improve the robustness of the algorithm in complex scenarios. Possible future directions include incorporating noise-handling mechanisms, utilizing multi-objective optimization to simultaneously consider different damage indicators, and integrating prior knowledge or physical constraints into the search process to guide the algorithm away from false-positive or false-negative detections.

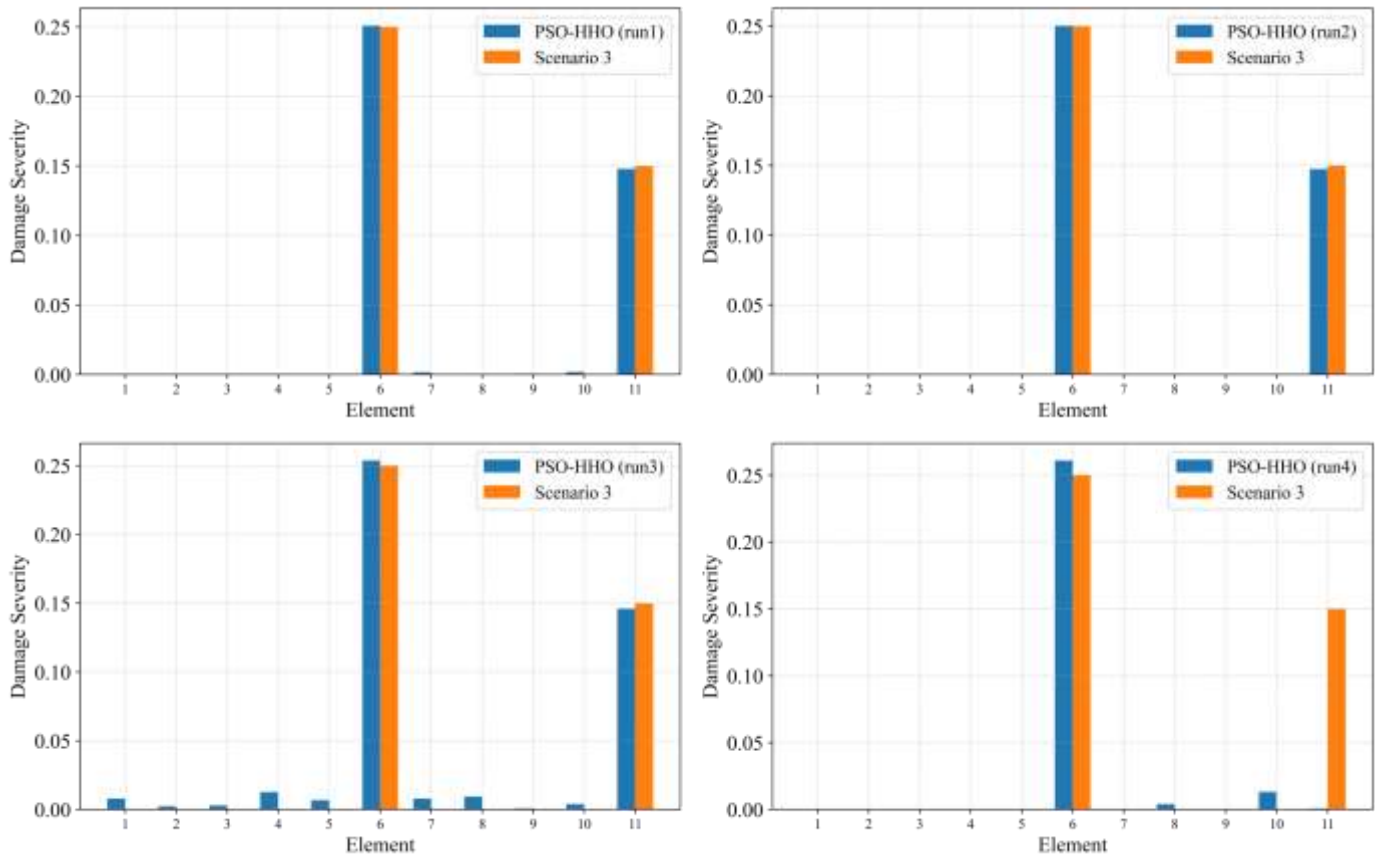

Fig. 18. The damage detection of each hybrid PSO-HHO algorithm run for scenario 3.

9. Conclusion

In this study, structural damage identification is performed by optimizing the objective function based on the modal parameters of the structure. To achieve this, a hybrid PSO-HHO algorithm is proposed and applied to detect damage under various scenarios. The results demonstrated the effectiveness of the hybrid approach in accurately identifying damage, outperforming individual algorithms and highlighting the value of integrating modal information for structural health monitoring. Based on the relevant findings of this research, the key observations can be categorized as follows:

1. The proposed hybrid PSO-HHO algorithm consistently outperforms the HHO and PSO algorithms in both damage scenarios. It achieves faster convergence, lower average cost function values, and greater stability in the final stages of optimization. This highlights the superior capability of the hybrid method, which identifies structural damage approximately 30% to 65% more accurately than the HHO algorithm.
2. The hybrid algorithm shows reliable performance in both single element and multiple element damage scenarios. Although deviations occur in the quantitative estimations, the method qualitatively identifies damage locations well. The algorithm demonstrates that in scenarios involving multiple simultaneous damages, careful tuning of its performance parameters is essential to ensure accurate results.

Statements & declarations

Author Contributions

Sayyed Hadi Alavi: Conceptualization, methodology, software, investigation, writing—original draft preparation, validation, writing—review and editing.

Amirhossein Pilehvaran: Conceptualization, methodology, software, investigation, validation, writing—review and editing.

Mohammadreza Mashayekhi: Conceptualization, methodology, software, investigation, writing—original draft preparation, validation, writing—review and editing, validation, supervision.

Acknowledgments

The authors thank their families for their constant support.

Funding

The author(s) received no financial support for the research, authorship, and publication of this article.

Declarations

The authors declare that they have no known competing financial interests or personal relationships that could have influenced the work reported in this paper.

Data availability

The data presented in this study are available on request from the corresponding author.

References

[1] Rincon, L. F., Moscoso, Y. M., Hamami, A. E. A., Matos, J. C., Bastidas-Arteaga, E. Degradation Models and Maintenance Strategies for Reinforced Concrete Structures in Coastal Environments under Climate Change: A Review. Buildings, 2024; 14 (3). doi:10.3390/buildings14030562.

[2] Feng, D., Feng, M. Q. Computer Vision for SHM of Civil Infrastructure: From Dynamic Response Measurement to Damage Detection – A Review. Engineering Structures, 2018; 156: 105–117. doi:10.1016/j.engstruct.2017.11.018.

[3] Asgari, A., Khabiri, A. Dynamic Analysis of Fatigue-Cracked Beams: The Nonlinear Response with the Analytical Method. Civil Engineering and Applied Solutions, 1: 89–100. doi:10.22080/ceas.2025.29000.1002.

[4] Tibaduiza Burgos, D. A., Gomez Vargas, R. C., Pedraza, C., Agis, D., Pozo, F. Damage Identification in Structural Health Monitoring: A Brief Review from Its Implementation to the Use of Data-Driven Applications. Sensors (Switzerland), 2020; 20 (3). doi:10.3390/s20030733.

[5] Kong, K., Dyer, K., Payne, C., Hamerton, I., Weaver, P. M. Progress and Trends in Damage Detection Methods, Maintenance, and Data-Driven Monitoring of Wind Turbine Blades – A Review. Renewable Energy Focus , 2023; 44: 390–412. doi:10.1016/j.ref.2022.08.005.

[6] Doebling, S. W. S., Farrar, C. R. C., Prime, M. B. M., Shevitz, D. W. D. Damage Identification and Health Monitoring of Structural and Mechanical Systems from Changes in Their Vibration Characteristics: A Literature Review. Los Alamos National Laboratory, 1996; doi:10.2172/249299.

[7] Xiang, Z., Wang, L., Zhou, M. Suppressing Damage Identification Errors from Selected Natural Frequencies and Mode Shape Points. Inverse Problems in Science and Engineering, 2012; 20 (7): 871–890. doi:10.1080/17415977.2011.589902.

[8] Abe, M. Structural Damage Detection by Natural Frequencies. In 37th Structure, Structural Dynamics and Materials Conference. American Institute of Aeronautics and Astronautics: Reston, Virigina, 1996; pp 1064–1069. doi:10.2514/6.1996-1440.

[9] Kaveh, A., Zolghadr, A. An Improved CSS for Damage Detection of Truss Structures Using Changes in Natural Frequencies and Mode Shapes. Advances in Engineering Software, 2015; 80: 93–100. doi:10.1016/j.advengsoft.2014.09.010.

[10] Cawley, P., Adams, R. D. The Location of Defects in Structures from Measurements of Natural Frequencies. The Journal of Strain Analysis for Engineering Design, 1979; 14 (2): 49–57. doi:10.1243/03093247V142049.

[11] Adams, R. D., Cawley, P., Pye, C. J., Stone, B. J. Vibration Technique for Non-Destructively Assessing the Integrity of Structures. J Mech Eng Sci, 1978; 20 (2): 93–100. doi:10.1243/jmes_jour_1978_020_016_02.

[12] Ciambella, J., Pau, A., Vestroni, F. Modal Curvature-Based Damage Localization in Weakly Damaged Continuous Beams. Mechanical Systems and Signal Processing, 2019; 121: 171–182. doi:10.1016/j.ymssp.2018.11.012.

[13] Chu, S. Y., Wu, R. L. A Normalized-Relative-Displacement-Vibration-Shape (NRDVS)-Based Structural Damage Assessment Scheme. Journal of Structural Integrity and Maintenance, 2018; 3 (3): 150–159. doi:10.1080/24705314.2018.1492667.

[14] Liu, Y. Research on Bridge Damage Identification Method Based on Dynamic Characteristics. Journal of Engineering Research and Reports, 2023; 25 (8): 87–93. doi:10.9734/jerr/2023/v25i8961.

[15] Yoo, S.-H. Damage Detection of Shear Building Structures Using Dynamic Response. Journal of the Korea institute for structural maintenance and inspection, 2014; 18 (3): 101–107. doi:10.11112/jksmi.2014.18.3.101.

[16] Hsieh, K. H., Halling, M. W., Barr, P. J., Robinson, M. J. Structural Damage Detection Using Dynamic Properties Determined from Laboratory and Field Testing. Journal of Performance of Constructed Facilities, 2008; 22 (4): 238–244. doi:10.1061/(asce)0887-3828(2008)22:4(238).

[17] Sun, G., Liu, C., Zhang, S., Hao, E. Three-Step Damage Identification Method Based on Dynamic Characteristics. Transactions of Tianjin University, 2014; 20 (5): 379–384. doi:10.1007/s12209-014-2115-z.

[18] Feng, D., & Feng, M. Q. Computer vision for SHM of civil infrastructure: From dynamic response measurement to damage detection–A review. Engineering Structures, 2018; 156:105-117. Doi: 10.1016/j.engstruct.2017.11.018.

[19] Pothisiri, T., Hjelmstad, K. D. Structural Damage Detection and Assessment from Modal Response. Journal of Engineering Mechanics, 2003; 129 (2): 135–145. doi:10.1061/(asce)0733-9399(2003)129:2(135).

[20] Huynh, D., He, J., Tran, D. Damage Location Vector: A Non-Destructive Structural Damage Detection Technique. Computers and

Structures, 2005; 83 (28-30): 2353–2367. doi:10.1016/j.compstruc.2005.03.029.

[21] Escobar, J. A., Sosa, J. J., Gómez, R. Structural Damage Detection Using the Transformation Matrix. Computers and Structures, 2005; 83 (4–5): 357–368. doi:10.1016/j.compstruc.2004.08.013.

[22] Magacho, E. G., Jorge, A. B., Gomes, G. F. Inverse Problem Based Multiobjective Sunflower Optimization for Structural Health Monitoring of Three-Dimensional Trusses. Evolutionary Intelligence, 2023; 16 (1): 247–267. doi:10.1007/s12065-021-00652-4.

[23] Mashayekhi, M., Shirpour, A., Sadeghi, R. Finding Optimum Parameters of Passive Tuned Mass Damper by PSO, WOA, and Hybrid PSO-WOA (HPW) Algorithms. Journal of Soft Computing in Civil Engineering, 2023; 7 (4): 72–92. doi:10.22115/SCCE.2023.352340.1489.

[24] Ghaemifard, S., Ghannadiasl, A. Usages of Metaheuristic Algorithms in Investigating Civil Infrastructure Optimization Models; a Review. AI in Civil Engineering, 2024; 3 (1). doi:10.1007/s43503-024-00036-4.

[25] Sahoo, B., Maity, D. Damage Assessment of Structures Using Hybrid Neuro-Genetic Algorithm. Applied Soft Computing Journal, 2007; 7 (1): 89–104. doi:10.1016/j.asoc.2005.04.001.

[26] Aval, S. B. B., Mohebian, P. A Novel Optimization Algorithm Based on Modal Force Information for Structural Damage Identification. International Journal of Structural Stability and Dynamics, 2021; 21 (7). doi:10.1142/S0219455421501005.

[27] Abdolkhani, A., Raoufi, R. Structural Modal Identification and Damage Detection with Incomplete Data Utilized by Genetic Algorithm Optimization. Structures, 2023; 55: 16–27. doi:10.1016/j.istruc.2023.06.009.

[28] Gökdağ, H., Yildiz, A. R. Structural Damage Detection Using Modal Parameters and Particle Swarm Optimization. Materialpruefung/Materials Testing, 2012; 54 (6): 416–420. doi:10.3139/120.110346.

[29] Chandrupatla, T., Belegundu, A. Introduction to finite elements in engineering. London: Pearson; 2021. doi:10.1017/9781108882293.

[30] Kaveh, A., Dadras, A. Structural Damage Identification Using an Enhanced Thermal Exchange Optimization Algorithm. Engineering Optimization, 2018; 50 (3): 430–451. doi:10.1080/0305215X.2017.1318872.

[31] Zhu, J. J., Huang, M., Lu, Z. R. Bird Mating Optimizer for Structural Damage Detection Using a Hybrid Objective Function. Swarm and Evolutionary Computation, 2017; 35: 41–52. doi:10.1016/j.swevo.2017.02.006.

[32] Zamani, F., Alavi, S. H., Mashayekhi, M., Noroozinejad Farsangi, E., Sadeghi-Movahhed, A., Majdi, A. Optimum Design of Double Tuned Mass Dampers Using Multiple Metaheuristic Multi-Objective Optimization Algorithms under Seismic Excitation. Frontiers in Built Environment, 2025; 11. doi:10.3389/fbuil.2025.1559530.

[33] Minh, H. Le, Sang-To, T., Abdel Wahab, M., Cuong-Le, T. A New Metaheuristic Optimization Based on K-Means Clustering Algorithm and Its Application to Structural Damage Identification. Knowledge-Based Systems, 2022; 251 (109189). doi:10.1016/j.knosys.2022.109189.

[34] Tran-Ngoc, H., Khatir, S., Ho-Khac, H., De Roeck, G., Bui-Tien, T., Abdel Wahab, M. Efficient Artificial Neural Networks Based on a Hybrid Metaheuristic Optimization Algorithm for Damage Detection in Laminated Composite Structures. Composite Structures, 2021; 262 (113339). doi:10.1016/j.compstruct.2020.113339.

[35] Zacharakis, I., Giagopoulos, D. Vibration-Based Damage Detection Using Finite Element Modeling and the Metaheuristic Particle Swarm Optimization Algorithm. Sensors, 2022; 22 (14). doi:10.3390/s22145079.

[36] Kareem, S. W., Hama Ali, K. W., Askar, S., Xoshaba, F. S., Hawezi, R. Metaheuristic Algorithms in Optimization and Its Application: A Review. JAREE (Journal on Advanced Research in Electrical Engineering), 2022; 6 (1). doi:10.12962/jaree.v6i1.216.

[37] Abbasi, M. H., Moradi, H. Optimum Design of Tuned Mass Damper via PSO Algorithm for the Passive Control of Forced Oscillations in Power Transmission Lines. SN Applied Sciences, 2020; 2 (5). doi:10.1007/s42452-020-2677-4.

[38] Mashayekhi, M. R., Mosayyebi, S. A New Hybrid Harris Hawks Optimization (HHO) and Particle Swarm Optimization (PSO) Algorithm for the Design of Castellated Beams. Asian Journal of Civil Engineering, 2023; 24 (7): 2121–2139. doi:10.1007/s42107-023-00630-4.

[39] Coello Coello, C. A., Pulido, G. T., Lechuga, M. S. Handling Multiple Objectives with Particle Swarm Optimization. IEEE Transactions on Evolutionary Computation, 2004; 8 (3): 256–279. doi:10.1109/TEVC.2004.826067.

[40] Kennedy J, Eberhart R. Particle swarm optimization. In: Proceedings of ICNN'95 – International Conference on Neural Networks; 1995 Nov 27–Dec 1; Perth, Australia. Vol. 4. p. 1942–8.

[41] Mashayekhi, M., Harati, M., Estekanchi, H. E. Development of an Alternative PSO-Based Algorithm for Simulation of Endurance Time Excitation Functions. Engineering Reports, 2019; 1 (3). doi:10.1002/eng2.12048.

[42] lu, junhui, Zhang, L., Yue, Y. A Particle Swarm Optimization Algorithm with Dynamic Weights. In Second International Conference on Electronic Information Technology (EIT 2023), SPIE; Xiao, W., Leng, L., Eds.; 2023; p 142. doi:10.1117/12.2685758.

[43] Heidari, A. A., Mirjalili, S., Faris, H., Aljarah, I., Mafarja, M., Chen, H. Harris Hawks Optimization: Algorithm and Applications. Future Generation Computer Systems, 2019; 97: 849–872. doi:10.1016/j.future.2019.02.028.

[44] Alabool, H. M., Alarabiat, D., Abualigah, L., Heidari, A. A. Harris Hawks Optimization: a comprehensive review of recent variants and applications. Neural Computing and Applications. 2021; 33:8939–80. doi:10.1007/s00521-021-05720-5.

[45] Clerc, M., Kennedy, J. The Particle Swarm-Explosion, Stability, and Convergence in a Multidimensional Complex Space. IEEE Transactions on Evolutionary Computation, 2002; 6 (1): 58–73. doi:10.1109/4235.985692.

[46] Devarapalli, R., Kumar, V. Power System Oscillation Damping Controller Design: A Novel Approach of Integrated HHO-PSO Algorithm. Archives of Control Sciences, 2021; 31 (3): 553–591. doi:10.24425/acs.2021.138692.

[47] Ashfaq, R., Sajjad, I. A. Multiobjective optimal power flow (MO-OPF) using hybrid Harris Hawk–Particle Swarm Optimization algorithm (HHO–PSO). In: 2023 6th International Conference on Energy Conservation and Efficiency (ICECE); 2023 Mar 15–16; Lahore, Pakistan. p. 1–6. doi:10.1109/ICECE58062.2023.10092489.

[48] Murugesan, S., Suganyadevi, M. V. Performance Analysis of Simplified Seven-Level Inverter Using Hybrid HHO-PSO Algorithm for Renewable Energy Applications. Iranian Journal of Science and Technology - Transactions of Electrical Engineering, 2024; 48 (2): 781–801. doi:10.1007/s40998-023-00676-9.

[49] Laier, J. E., Villalba, J. D. Ensuring Reliable Damage Detection Based on the Computation of the Optimal Quantity of Required Modal Data. Computers and Structures, 2015; 147: 117–125. doi:10.1016/j.compstruc.2014.09.020.

[50] Hibbeler, R. C., Tan, K. H. Structural analysis. Harlow (UK): Pearson Prentice Hall; 2006.